Published in final edited form as:
Magn Reson Med. 2008 December ; 60(6): 1269–1275. doi:10.1002/mrm.21816.

In Vivo Serial Evaluation of Super-Paramagnetic Iron-Oxide Labeled Stem Cells by Off-Resonance Positive Contrast

Yoriyasu Suzuki, MD[1,2], **Charles H. Cunningham, PhD**[3], **Ken-ichiro Noguchi, MD**[4], **Ian Y. Chen**[5], **Irving L. Weissman, MD**[6], **Alan C. Yeung, MD**[1], **Robert C. Robbins, MD**[4], and **Phillip C. Yang, MD**[1,*]

[1]Division of Cardiovascular Medicine, Department of Medicine, Okazaki City Hospital, Okazaki, Aichi, Japan

[2]Department of Cardiology, Okazaki City Hospital, Okazaki, Aichi, Japan

[3]Department of Medical Biophysics, University of Toronto, Canada

[4]Department of Cardiothoracic Surgery, Stanford University, Stanford, California, USA

[5]Department of Bioengineering, Stanford University, Stanford, California, USA

[6]Department of Pathology, Stanford University, Stanford, California, USA

Abstract

Magnetic resonance imaging (MRI) is emerging as a diagnostic modality to track iron-oxide labeled stem cells. This study investigates whether an off-resonance (OR) pulse sequence designed to generate positive contrast at 1.5-Tesla can assess location, quantity and viability of delivered stem cells *in vivo*. Using mouse embryonic stem cell transfected with luciferase reporter gene (*luc*-mESC), multimodality validation of OR signal was conducted to determine whether engraftment parameters of superparamagnetic iron-oxide labeled *luc*-mESC (SPIO-*luc*-mESC) could be determined after cell transplantation into the mouse hind limb. A significant increase in signal- and contrast-to-noise of the *SPIO-luc-mESC* was achieved by OR technique when compared to GRE sequence. A significant correlation between the quantity of SPIO-*luc*-mESC and OR signal was observed immediately after transplantation (R^2=0.74, p<0.05). The assessment of transplanted cell viability by bioluminescence imaging (BLI) showed significant increase of luciferase activities by day 16 while MRI signal showed no difference. No significant correlation between BLI and MRI signals of cell viability was observed.

In conclusion, using off-resonance sequence, the precise localization and quantitation of SPIO-labeled stem cells in both space and time were possible. However, off-resonance sequence did not allow evaluation of cell viability.

Keywords

positive contrast; cellular MRI; embryonic stem cell

Introduction

Growing evidence from preclinical and clinical studies suggests that stem cell therapy may provide a viable therapeutic alternative to restore the target organ (1–5). Development of a

*Address for correspondence: Phillip C. Yang, Stanford University Medical Center, 300 Pasteur Drive, Room H-2157, Stanford, CA 94305-5233, USA. E-mail: pyang@cvmed.stanford.edu, Phone; (650) 498-8008, Fax; (650) 724-4034.

sensitive, noninvasive imaging technology to track the engraftment of transplanted stem cells will be critical in monitoring therapeutic efficacy.

Imaging modalities including single-photon emission computed tomography (SPECT), positron emission tomography (PET), optical fluorescence, and magnetic resonance imaging (MRI) have all been implemented to evaluate the transplanted stem cells (6–13). MRI using super paramagnetic iron oxide (SPIO) cell labeling techniques is emerging as the main diagnostic modality to track the transplanted stem cells. This technique exploits the T_2* properties of SPIO agents to generate negative (hypointense) MRI contrast when the nanoparticles are compartmentalized within the cells. Although MRI of SPIO-labeled stem cells is a simple technique with robust and reliable results, a fundamental drawback of negative MRI contrast agents is that the signal is often confounded by the presence of artifacts generated by hemorrhage, air, and partial-volume effects (14–17). In order to address these issues, techniques to generate positive contrast to enhance signal- and contrast-to noise ratios (SNR and CNR) of the labeled stem cells have been developed. Our laboratory has reported off-resonance MRI (OR) of SPIO-labeled mouse embryonic stem cells to generate positive contrast through suppression of background tissue (18). Several techniques have been described to achieve similar positive contrast from SPIO-labeled cells (19–21).

Some of the fundamental parameters of stem cell engraftment following delivery into a target organ consist of cell location, quantity, and survival. Validation of stem cell engraftment parameters using conventional reporter gene techniques (eg, green fluorescent protein) or a thymidine analogue (eg, bromodeoxyuridine [BrDU]) has depended mostly on postmortem immunohistological analysis. Recently optical imaging methods such as bioluminescence imaging (BLI) and fluorescence imaging have been used for stem cell tracking. Successful *in vivo* evaluation of stem cell distribution and engraftment has been reported in small-animal studies. Using light generated by the enzyme luciferase and sensitive low-light imaging systems, BLI allows detection of small numbers of transplanted cells within the tissues of small animal models reaching sensitivity of 10^{-15}–10^{-17} mole/L (22–24). Specific targeting of luciferase transgene expression in restricted cells and tissues of interest has allowed the localization and tracking of cell fate for studying a variety of disease processes. Although the survival of stem cells injected into the myocardium using PET and BLI has been demonstrated, the specific engraftment kinetics of stem cells could not be fully delineated (9,25).

The aim of this study is to determine whether positive contrast generated by OR sequence provides useful information to monitor the engraftment of transplanted stem cells. Critical biological information following cell delivery regarding location, quantity, and survival of transplanted stem cells have been investigated systematically using multimodality validation including molecular reporter gene signal detected by BLI as a standard to assess stem cell survival *in vivo*.

Methods

Cell culture and Cell labeling

Cell culture—The mESC were maintained in an undifferentiated state on a feeder layer of irradiated mouse fibroblasts with maintenance medium containing Dulbecco modified Eagle medium (Invitrogen, Carlsbad, CA) supplemented with 15% Fetal Bovine Serum (Hyclone, Logan, UT), 0.1 mM 2-mercaptoethanol (Sigma, St. Louis, MO), 0.1 mM non-essential amino acids (Invitrogen), 1% penicillin/streptomycin (Invitrogen), 2 mM L-glutamine (Invitrogen), and 1000U/mL mouse leukemia inhibitory factor (LIF)(ESGRO, Chemicon, Temecula, CA) at 37°C as described previously (17). The stable mESC transfected with

Click Beetle Red luciferase reporter gene (*luc*-mESC, courtesy of Dr. Joseph C. Wu, Stanford University, Stanford, CA) were used.

Cell labeling—To label *luc*-mESC, we used the commercially available ferumoxides suspension (Feridex IV, Berlex Laboratories, Wayne, NJ) which contains particles approximately 80 to 150 nm in size and has a total iron content of 11.2 mg Fe/mL. Clinical grade protamine sulfate (PS, American Pharmaceuticals Partner, Schaumburg, IL) was prepared as a stock solution of 1 mg/mL in distilled water. Ferumoxides (100μg Fe/mL) was put into a tube containing serum-free RPMI 1640 medium (Invitrogen) containing 25 mM HEPES and L-glutamine. PS was added to that solution at a concentration of 12μg/mL. The solution containing ferumoxides and PS was mixed for 5 to 10 minutes. Equal volume of labeling solution was added to the existing medium in the mESC culture and incubated for 12–24 hours (15,17). The final concentration of Ferumoxides and PS in the cell culture medium was 50μg Fe/mL and 6μg/mL, respectively.

Animal preparation and cell injection

A total of 11 healthy female SCID mice (8–10 weeks old) were studied under a protocol approved by the Stanford University Administrative Panel on Laboratory Animal Care. After inhalational anesthetic induction, a 50μL volume from each dilution of SPIO-labeled *luc*-mESC (SPIO-*luc*-mESC) suspension was injected into both hind limbs of each mouse using 27G needle. For quantitation of *in vivo* MRI using OR, three different cell populations of SPIO-*luc*-mESC were injected (1, 3, 5×10^6, n=3/group). To assess the correlation between BLI and iron oxide-based cellular MRI, 3×10^6 viable SPIO-*luc*-mESC and 3×10^6 formalin-fixed non-viable SPIO-*luc*-mESC SPIO were transplanted into a total of 8 mice. Three mice were euthanized at day 1 and 8 mice were euthanized at day 16. We confirmed by trypan blue exclusion that all SPIO-*luc*-mESC were dead after formalin fixation.

In vivo MR imaging

In vivo MRI at 1.5T-MR scanner (Signa, GE Medical Systems, Milwaukee, WI) using a 3-inch surface coil was performed to correlate BLI and Off-resonance MRI (OR) of SPIO-*luc*-mESC on 1, 4, 7, 10, and 16 days after cell transplantation. The mice were anesthetized with intraperitoneal injection of Ketamine (100mg/kg) and Xylazine (20mg/kg), allowed to breathe spontaneously, and imaged in a head-first prone position. In order to ensure positional consistency and orientation of the hind limb for serial imaging, the angle between hind limb and tail was set at 45–60 degree and the center of the 3-inch surface coil was placed at the center of both hind limbs. After localization, gradient recalled echo (GRE) images acquired in a series of 9 to 10 contiguous coronal slices provided complete coverage of the murine hind limb (TR=100msec, TE=10msec, Flip angle=30°, FOV=8×8cm, slice thickness=1mm, slice gap=0mm, matrix=256×256, NEX=4).

The GRE sequence was followed by OR acquisition to generate positive contrast. The OR sequence enables selective T2-weighted imaging of the off-resonance water frequencies, by employing a narrow RF bandwidth (1 kHz passband) tuned to roughly −800 Hz from the endogenous tissue water, combined with refocusing and a short readout. Our off-resonance sequence utilizes spectrally selective RF pulses to excite and refocus the off-resonance water surrounding the labeled cells while minimizing on-resonance signal. By matching the profiles of a 90° excitation and a 180° refocusing pulse, a spin-echo sequence with million-fold (120 dB) suppression of on-resonance water was designed (18). This generates positive contrast from the hydrogen protons adjacent to SPIO-*luc*-mESC in order to better identify and estimate the volume of the labeled cells. Projectional OR images were obtained in a two minute time window at negative frequency offsets (TR=800msec, TE=14msec, FOV=10cm, 8-ms readout, and matrix=256×128 with 2 DFT encoding) (18,26).

In vivo optical bioluminescence imaging

To evaluate the longitudinal viability and proliferation of transplanted cells, BLI was performed serially on days 1, 4, 7, 10, and 16 following cell transplantation using the In Vivo Imaging System (Caliper Life Sciences, Hopkinton, MA). Images were acquired using 1 to 10-minute intervals until peak signal was observed and analyzed using commercially available software (Caliper Life Sciences, Hopkinton, MA). Luciferase generates most light activity 15–20 minutes after intraperitoneal injection of substrate luciferin at a dose of 30 mg/kg body weight (9).

Imaging data analysis

In Vivo MRI Signal Analysis—For *in vivo* OR assessment of cell location, the SNR and CNR obtained from OR and GRE acquisition of SPIO-*luc*-mESC were calculated. SNR was defined as the signal intensity generated from SPIO-labeled cells relative to the standard deviation of the background noise. CNR was defined as the signal difference relative to a reference signal in the hind limb. The signal measurements per region of interest (ROI) were obtained by manual tracing using Image J (NIH, Bethesda, MD) and included only pixels with a per voxel SNR threshold greater than 6. The signal volume of GRE images was measured by summation of hypointense area of each slice. The OR signal enhancement area was obtained by measuring the area of projectional OR image. Precision of cell number quantification characterized as 'sensitivity' was defined as the relative increase in cell number elevating the contrast area or SNR by a quantity equivalent to the 95% confidence interval of the slope under linear transformation ($\Delta x/x > 2\sigma_B/B$, expressed as a percentage, which is derivable by equating $y = A+B(x+\Delta x)$ and $y = A + (B + 2\sigma_B)x$) (26).

In vivo BLI data analysis—Quantitative analysis of bioluminescence images was performed by manual drawing of ROIs on the hind limb projection image. The signal within the ROI was integrated using the IVIS imaging analysis software (Caliper Life Sciences, Hopkinton, MA).

Statistical Analysis

All statistical analysis was performed by using SPSS 13.0 (SPSS Inc., Chicago, IL). All data are expressed as mean +/− standard deviation (SD). The correlation between BLI activities and MR signals was analyzed by simple linear regression with 95% confidence intervals. Comparison of BLI activities, and MR signals from same animals between different time points were made using repeated-measures ANOVA technique. A p value less than 0.05 was considered statistically significant.

Results

In vivo MRI of stem cell location and quantity

Representative magnetic resonance images by conventional GRE and OR techniques are shown in Fig. 1A–D. Both SNR and CNR by OR acquisition are significantly higher than those by GRE acquisition facilitating accurate localization of the labeled cells as shown in Fig. 1E and F. The significant linear correlations between the quantities of injected SPIO-*luc*-mESC and the signal areas by OR and GRE techniques are observed in Fig. 2A–C (OR; R^2=0.79, p<0.0001, GRE; R^2=0.68, p<0.0001, respectively). The sensitivities of both GRE and OR techniques are shown in Table 1.

In vivo evaluation of stem cell viability

BLI—Representative serial *in vitro* and *in vivo* bioluminescence images are shown in Fig. 3A and C. *In vitro* estimation of bioluminescence activities demonstrates a significant linear

correlation between the number of *luc*-mESC and bioluminescence signal (R^2=0.94, p<0.001) as shown in Fig. 3B. Furthermore, clear visual distinction between viable and non-viable *luc*-mESC is made *in vivo* as the bioluminescence measurements of non-viable *luc*-mESC in the contralateral hind limb demonstrate no luciferase activity as shown in Fig. 3C (arrow: live cells and arrow head: dead cells, respectively). The mean bioluminescence signal of viable SPIO-*luc*-mESC increases over time as shown in Fig. 3D. Although the mean bioluminescence signal of viable SPIO-*luc*-mESC demonstrates no significant change from day 1 to 10, a significant increase is seen on day 16 following transplantation (p<0.001) indicating proliferation of the transplanted mESC.

MRI—Representative serial magnetic resonance images of viable and non-viable cells detected by GRE and OR techniques during the 16-day period are shown in Fig. 1C and D. The analysis of the mean signal area by OR technique demonstrates no difference between viable and non-viable *luc*-mESC at any time. Furthermore, the analysis of mean signal volume of labeled *luc*-mESC generated by GRE technique shows no difference. Finally, the bioluminescence activity and magnetic resonance signal area by GRE and OR techniques demonstrate no correlation at any time point as demonstrated. These data suggest that both GRE and OR techniques did not detect cell viability or proliferation.

Discussion

This study addresses some of the key challenges to *in vivo* MRI evaluation of cell engraftment parameters including localization, quantification, and viability of the transplanted cells. First, *in vivo* OR signal of SPIO-labeled cells demonstrated significantly higher SNR and CNR compared to standard GRE signal allowing cell localization following transplantation. Second, significant linear correlations between the quantity of transplanted SPIO-luc-mESC and the signal areas by both negative and positive-contrast methods were observed enabling precise *in vivo* quantification of cells immediately following delivery. Third, the survival of SPIO-luc-mESC monitored by BLI demonstrated a lack of correlation with the MRI signal. Thus, both *in vivo* OR and GRE imaging of SPIO-labeled cells did not demonstrate sensitivity to cellular viability.

Localization

Robust detection of SPIO-labeled stem cells delivered into the tissue is possible with clinically available SPIO agents such as Feridex IV. These capabilities may enable longitudinal monitoring of transplanted stem cells as demonstrated by *in vivo* MR tracking of SPIO-labeled dendritic cells in human (27). However, signal voids generated from iron oxide particles present the challenge of distinguishing SPIO-labeled cells from the surrounding air, hemorrhage, necrosis, and macrophages. Specifically, in cardiac imaging, the air-tissue interface with the lung can be problematic in generating accurate localization of the labeled cells. In this study, OR signal of SPIO-labeled cells demonstrated significantly higher SNR and CNR compared to standard GRE signal. This observation suggests that our OR technique addresses these issues by providing positive contrast to enable accurate detection of the labeled cells immediately after cell transplantation. Similarly other groups have reported alternative MRI methods for positive contrast visualization of superparamagnetic objects (21,28,29). First, Gradient echo Acquisition for Superparamagnetic particles/suscePtibility (GRASP) demonstrated positive contrast from the area surrounding susceptibility-generating objects (21). However, this technique necessitates the modification of pulse sequence and is limited to GRE. Second, spectrally selective RF pulses to pre-saturate on-resonant water have been reported. Inversion recovery of on-resonance water suppression (IRON) results in voxels with hyperintense signal from SPIO-labeled cells with background attenuation of 20 dB (28). Finally, a post processing

method to generate positive-contrast employing susceptibility-gradient mapping (SGM) has been developed (29). No special pulse sequence, RF pulse, or acquisition technique is required in this SGM method to generate hyperintense signal to allow detection of SPIO-labeled cells.

Quantification

In our study, the signal by GRE technique demonstrated a strong correlation with estimated cell number. By regression analysis, GRE technique appears to be more sensitive than OR technique to cell quantity since the dynamic range of the area change is greater over a similar range of cell numbers. However, it will be difficult to take advantage of this sensitivity of GRE technique in *in vivo* studies because the negative-contrast generated by air surrounding the tissue confounds the majority of the hind-limb signal. The obvious advantage of GRE method, with higher sensitivity to smaller cell numbers, may not necessarily be advantageous when looking for longitudinal changes in the cell numbers in regions with competing negative signals. Although MRI of SPIO-labeled stem cells are simple to implement with robust and reliable results, the major drawback is due to the derivation of the signal from non-specific cellular uptake of iron oxide nanoparticles. The sensitivity of OR technique can be enhanced by factors such as coil design, spatial resolution, and field strength. The current OR technique is limited by projectional background suppression requiring a large volume of water to be suppressed. Potential improvements include slice selection capability and shorter duration of the frequency selective RF excitations. Using the same OR method, Gd-DTPA mediated elevation of signal area and SNR has been reported to facilitate the detection of cell quantity as low as 25,000 cells (26). This suggests a possible mechanism of OR signal enhancement associated with cell proliferation. As the cells proliferate, the constant number of nanoparticles is merely divided among the daughter cells leading to a dilution of iron, which should lead to changes in the local susceptibility to generate T1 contrast signal by both OR and GRE techniques. This technique may also improve the sensitivity of longitudinal monitoring of transplanted stem cells.

Viability

Previous studies of the survival of transplanted neonatal cardiomyocyte showed that at day 1, TUNEL indices increased to 32.1%, remained high at day 4 averaging 9.8%, and by day 7 decreased to 1.0% (30). On the other hand, in the studies using mESC transfected reporter gene and optical imaging, bioluminescence activities increased progressively from week 1 to week 4 after cell transplantation, which indicated transplanted cell survival and proliferation in the host (25,31). Similarly, in our study, the survival of SPIO-*luc*-mESC determined by bioluminescence activity of luciferase gene expression decreased to one-third at day 4 and 7 and increased to 50-fold at day 16. This observation suggested that the mESC transplanted in the hind limb proliferated. Using correlation curve between the number of SPIO-*luc*-mESC and MRI signal, 2 to 3-fold changes in viable cell number should have been detected. However, the signal generated from MRI and BLI studies did not correlate.

Complementary modalities

High sensitivity of PET and optical imaging may be more suitable to detect signal generated from specific molecular processes. Optical BLI uses light generated by the enzyme luciferase, which does not require external light excitation and emits light in yellow to green wavelengths with the presence of luciferin, ATP, magnesium, and oxygen. The camera of the bioluminescence imaging system is capable of detecting a minimum radiance of 100 photons per second per cm^2 per steridian (photons/second/cm^2/sr) and achieves a minimal image pixel resolution of 50μm (9). High reproducibility (within ± 8% standard deviation from mean values) and detection sensitivity of this system for monitoring luciferase reporter

gene expression has been demonstrated *in vivo* (32). However, these imaging modalities are limited by poor spatial and temporal resolution and penetration (33). MRI, on the other hand, has the advantage of high spatial and temporal resolution with exquisite tissue contrast. Novel imaging sequences, higher magnetic fields, hardware development, targeted contrast agents, and reporter gene technology have been developed to amplify the cellular signal (18,20,21,34–39). These approaches are pursued in our and other laboratories to enable a more sensitive *in vivo* MRI to combine cellular and molecular signals with precise 3-D and 4-D characterization of the surrounding cardiovascular function and morphology (40,41).

Study Limitation

This study was investigated within a time window of 16 days. Thus, our findings were limited to short-term findings of cellular MRI following transplantation into a target organ.

Conclusion

The positive contrast has been found to enable significant increase in SNR and CNR over standard GRE acquisition. Furthermore, significant linear correlation between the quantity of transplanted SPIO-luc-mESC and the signal areas by both negative and positive-contrast methods were observed. These observations suggest that positive contrast generated by off resonance method allowed reliable detection and quantification of the SPIO-labeled cells following delivery into the target organ. However, the survival signal of SPIO-*luc*-mESC monitored by BLI did not correlate with the MRI signal.

Acknowledgments

This work was supported by National Institute of Health, NHLBI 5K18HL87198-2 and American Heart Association, Beginning Grant-in-Aid. We thank Sally Zhang and Pratima Kundu for their technical assistance.

References

1. Orlic D, Kajstura J, Chimenti S, Jakoniuk I, Anderson SM, Li B, Pickel J, McKay R, Nadal-Ginard B, Bodine DM, Leri A, Anversa P. Bone marrow cells regenerate infarcted myocardium. Nature. 2001; 410(6829):701–705. [PubMed: 11287958]
2. Schachinger V, Assmus B, Britten MB, Honold J, Lehmann R, Teupe C, Abolmaali ND, Vogl TJ, Hofmann WK, Martin H, Dimmeler S, Zeiher AM. Transplantation of progenitor cells and regeneration enhancement in acute myocardial infarction: final one-year results of the TOPCARE-AMI Trial. J Am Coll Cardiol. 2004; 44(8):1690–1699. [PubMed: 15489105]
3. Assmus B, Honold J, Schachinger V, Britten MB, Fischer-Rasokat U, Lehmann R, Teupe C, Pistorius K, Martin H, Abolmaali ND, Tonn T, Dimmeler S, Zeiher AM. Transcoronary transplantation of progenitor cells after myocardial infarction. N Engl J Med. 2006; 355(12):1222–1232. [PubMed: 16990385]
4. Lunde K, Solheim S, Aakhus S, Arnesen H, Abdelnoor M, Egeland T, Endresen K, Ilebekk A, Mangschau A, Fjeld JG, Smith HJ, Taraldsrud E, Grogaard HK, Bjornerheim R, Brekke M, Muller C, Hopp E, Ragnarsson A, Brinchmann JE, Forfang K. Intracoronary injection of mononuclear bone marrow cells in acute myocardial infarction. N Engl J Med. 2006; 355(12):1199–1209. [PubMed: 16990383]
5. Schachinger V, Erbs S, Elsasser A, Haberbosch W, Hambrecht R, Holschermann H, Yu J, Corti R, Mathey DG, Hamm CW, Suselbeck T, Assmus B, Tonn T, Dimmeler S, Zeiher AM. Intracoronary bone marrow-derived progenitor cells in acute myocardial infarction. N Engl J Med. 2006; 355(12): 1210–1221. [PubMed: 16990384]
6. MacLaren DC, Toyokuni T, Cherry SR, Barrio JR, Phelps ME, Herschman HR, Gambhir SS. PET imaging of transgene expression. Biol Psychiatry. 2000; 48(5):337–348. [PubMed: 10978717]

7. Wu JC, Inubushi M, Sundaresan G, Schelbert HR, Gambhir SS. Positron emission tomography imaging of cardiac reporter gene expression in living rats. Circulation. 2002; 106(2):180–183. [PubMed: 12105155]
8. Barbash IM, Chouraqui P, Baron J, Feinberg MS, Etzion S, Tessone A, Miller L, Guetta E, Zipori D, Kedes LH, Kloner RA, Leor J. Systemic delivery of bone marrow-derived mesenchymal stem cells to the infarcted myocardium: feasibility, cell migration, and body distribution. Circulation. 2003; 108(7):863–868. [PubMed: 12900340]
9. Wu JC, Chen IY, Sundaresan G, Min JJ, De A, Qiao JH, Fishbein MC, Gambhir SS. Molecular imaging of cardiac cell transplantation in living animals using optical bioluminescence and positron emission tomography. Circulation. 2003; 108(11):1302–1305. [PubMed: 12963637]
10. Hill JM, Dick AJ, Raman VK, Thompson RB, Yu ZX, Hinds KA, Pessanha BSBSS, Guttman MAMA, Varney TRTR, Martin BJBJ, Dunbar CECE, McVeigh ERER, Lederman RJRJ. Serial cardiac magnetic resonance imaging of injected mesenchymal stem cells. Circulation. 2003; 108(8):1009. [PubMed: 12912822]
11. Kraitchman DL, Heldman AW, Atalar E, Amado LC, Martin BJ, Pittenger MF, Hare JM, Bulte JW. In vivo magnetic resonance imaging of mesenchymal stem cells in myocardial infarction. Circulation. 2003; 107(18):2290–2293. [PubMed: 12732608]
12. Himes N, Min JY, Lee R, Brown C, Shea J, Huang X, Xiao YF, Morgan JP, Burstein D, Oettgen P. In vivo MRI of embryonic stem cells in a mouse model of myocardial infarction. Magn Reson Med. 2004; 52(5):1214–1219. [PubMed: 15508153]
13. Arai T, Kofidis T, Bulte JW, de Bruin J, Venook RD, Berry GJ, McConnell MV, Quertermous T, Robbins RC, Yang PC. Dual in vivo magnetic resonance evaluation of magnetically labeled mouse embryonic stem cells and cardiac function at 1.5 t. Magn Reson Med. 2006; 55(1):203–209. [PubMed: 16315206]
14. Frank JA, Miller BR, Arbab AS, Zywicke HA, Jordan EK, Lewis BK, Bryant LH Jr, Bulte JW. Clinically applicable labeling of mammalian and stem cells by combining superparamagnetic iron oxides and transfection agents. Radiology. 2003; 228(2):480–487. [PubMed: 12819345]
15. Arbab AS, Yocum GT, Kalish H, Jordan EK, Anderson SA, Khakoo AY, Read EJ, Frank JA. Efficient magnetic cell labeling with protamine sulfate complexed to ferumoxides for cellular MRI. Blood. 2004; 104(4):1217–1223. [PubMed: 15100158]
16. Walczak P, Kedziorek DA, Gilad AA, Lin S, Bulte JW. Instant MR labeling of stem cells using magnetoelectroporation. Magn Reson Med. 2005; 54(4):769–774. [PubMed: 16161115]
17. Suzuki Y, Zhang S, Kundu P, Yeung AC, Robbins RC, Yang PC. In vitro comparison of the biological effects of three transfection methods for magnetically labeling mouse embryonic stem cells with ferumoxides. Magn Reson Med. 2007; 57(6):1173–1179. [PubMed: 17534917]
18. Cunningham CH, Arai T, Yang PC, McConnell MV, Pauly JM, Conolly SM. Positive contrast magnetic resonance imaging of cells labeled with magnetic nanoparticles. Magn Reson Med. 2005; 53(5):999–1005. [PubMed: 15844142]
19. Seppenwoolde JH, Viergever MA, Bakker CJ. Passive tracking exploiting local signal conservation: the white marker phenomenon. Magn Reson Med. 2003; 50(4):784–790. [PubMed: 14523965]
20. Heyn C, Bowen CV, Rutt BK, Foster PJ. Detection threshold of single SPIO-labeled cells with FIESTA. Magn Reson Med. 2005; 53(2):312–320. [PubMed: 15678551]
21. Mani V, Briley-Saebo KC, Itskovich VV, Samber DD, Fayad ZA. Gradient echo acquisition for superparamagnetic particles with positive contrast (GRASP): sequence characterization in membrane and glass superparamagnetic iron oxide phantoms at 1.5T and 3T. Magn Reson Med. 2006; 55(1):126–135. [PubMed: 16342148]
22. Massoud TF, Gambhir SS. Molecular imaging in living subjects: seeing fundamental biological processes in a new light. Genes Dev. 2003; 17(5):545–580. [PubMed: 12629038]
23. Rice BW, Cable MD, Nelson MB. In vivo imaging of light-emitting probes. J Biomed Opt. 2001; 6(4):432–440. [PubMed: 11728202]
24. Contag CH, Ross BD. It's not just about anatomy: in vivo bioluminescence imaging as an eyepiece into biology. J Magn Reson Imaging. 2002; 16(4):378–387. [PubMed: 12353253]

25. Cao F, Lin S, Xie X, Ray P, Patel M, Zhang X, Drukker M, Dylla SJ, Connolly AJ, Chen X, Weissman IL, Gambhir SS, Wu JC. In vivo visualization of embryonic stem cell survival, proliferation, and migration after cardiac delivery. Circulation. 2006; 113(7):1005–1014. [PubMed: 16476845]
26. Foltz WD, Cunningham CH, Mutsaers AJ, Conolly SM, Stewart DJ, Dick AJ. Positive-contrast imaging in the rabbit hind-limb of transplanted cells bearing endocytosed superparamagnetic beads. J Cardiovasc Magn Reson. 2006; 8(6):817–823. [PubMed: 17060104]
27. de Vries IJ, Lesterhuis WJ, Barentsz JO, Verdijk P, van Krieken JH, Boerman OC, Oyen WJ, Bonenkamp JJ, Boezeman JB, Adema GJ, Bulte JW, Scheenen TW, Punt CJ, Heerschap A, Figdor CG. Magnetic resonance tracking of dendritic cells in melanoma patients for monitoring of cellular therapy. Nat Biotechnol. 2005; 23(11):1407–1413. [PubMed: 16258544]
28. Stuber M, Gilson WD, Schar M, Kedziorek DA, Hofmann LV, Shah S, Vonken EJ, Bulte JW, Kraitchman DL. Positive contrast visualization of iron oxide-labeled stem cells using inversion-recovery with ON-resonant water suppression (IRON). Magn Reson Med. 2007; 58(5):1072–1077. [PubMed: 17969120]
29. Liu W, Dahnke H, Jordan EK, Schaeffter T, Frank JA. In vivo MRI using positive-contrast techniques in detection of cells labeled with superparamagnetic iron oxide nanoparticles. NMR Biomed. 2008; 21(3):242–250. [PubMed: 17566968]
30. Zhang M, Methot D, Poppa V, Fujio Y, Walsh K, Murry CE. Cardiomyocyte grafting for cardiac repair: graft cell death and anti-death strategies. J Mol Cell Cardiol. 2001; 33(5):907–921. [PubMed: 11343414]
31. Li Z, Suzuki Y, Huang M, Cao F, Xie X, Connolly AJ, Yang PC, Wu JC. Comparison of reporter gene and iron particle labeling for tracking fate of human embryonic stem cells and differentiated endothelial cells in living subjects. Stem Cells. 2008; 26(4):864–873. [PubMed: 18218820]
32. Wu JC, Sundaresan G, Iyer M, Gambhir SS. Noninvasive optical imaging of firefly luciferase reporter gene expression in skeletal muscles of living mice. Mol Ther. 2001; 4(4):297–306. [PubMed: 11592831]
33. Auerbach MA, Schoder H, Hoh C, Gambhir SS, Yaghoubi S, Sayre JW, Silverman D, Phelps ME, Schelbert HR, Czernin J. Prevalence of myocardial viability as detected by positron emission tomography in patients with ischemic cardiomyopathy. Circulation. 1999; 99(22):2921–2926. [PubMed: 10359737]
34. Winter PM, Morawski AM, Caruthers SD, Fuhrhop RW, Zhang H, Williams TA, Allen JS, Lacy EK, Robertson JD, Lanza GM, Wickline SA. Molecular imaging of angiogenesis in early-stage atherosclerosis with alpha(v)beta3-integrin-targeted nanoparticles. Circulation. 2003; 108(18): 2270–2274. [PubMed: 14557370]
35. Sosnovik DE, Schellenberger EA, Nahrendorf M, Novikov MS, Matsui T, Dai G, Reynolds F, Grazette L, Rosenzweig A, Weissleder R, Josephson L. Magnetic resonance imaging of cardiomyocyte apoptosis with a novel magneto-optical nanoparticle. Magn Reson Med. 2005; 54(3):718–724. [PubMed: 16086367]
36. Nahrendorf M, Jaffer FA, Kelly KA, Sosnovik DE, Aikawa E, Libby P, Weissleder R. Noninvasive vascular cell adhesion molecule-1 imaging identifies inflammatory activation of cells in atherosclerosis. Circulation. 2006; 114(14):1504–1511. [PubMed: 17000904]
37. Louie AY, Huber MM, Ahrens ET, Rothbacher U, Moats R, Jacobs RE, Fraser SE, Meade TJ. In vivo visualization of gene expression using magnetic resonance imaging. Nat Biotechnol. 2000; 18(3):321–325. [PubMed: 10700150]
38. Weissleder R, Moore A, Mahmood U, Bhorade R, Benveniste H, Chiocca EA, Basilion JP. In vivo magnetic resonance imaging of transgene expression. Nat Med. 2000; 6(3):351–355. [PubMed: 10700241]
39. Genove G, DeMarco U, Xu H, Goins WF, Ahrens ET. A new transgene reporter for in vivo magnetic resonance imaging. Nat Med. 2005; 11(4):450–454. [PubMed: 15778721]
40. Yang PC, Xie E, Kundu P, Stein W, Drukker M, Weissman I, Wu JC, Robbins RC. In vivo molecular MRI of mouse embryonic stem cell viability. Proc Intl Soc Mag Reson Med. 2007; 15:1173.

41. Yamada M, Kundu P, Drukker M, Weissman I, Robbins RC, Yang PC. Manganese guided cellular MRI of human embryonic stem cell viability. Proc Intl Soc Mag Reson Med. 2007; 15:1198.

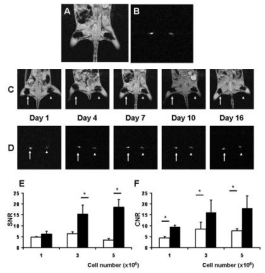

Figure 1. *In vivo* MR imaging

Representative *in vivo* MRI images. (A) GRE and (B) Off-Resonance imaging (OR). Serial *in vivo* MRI of SPIO-labeled mESC from 1–16 day after cell transplantation; (C) GRE and (D) OR (arrow: viable cells and arrowhead: non-viable cells). Signal-to-noise ratio (SNR) and contrast-to-noise ratio (CNR) of *in vivo* GRE vs. OR (white bar indicates GRE and black bar indicates OR, *$p<0.05$); (E) SNR; and (F) CNR.

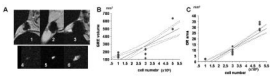

Figure 2. *In vivo* MRI of stem cell quantity

Representative MR images of GRE (1–3) and OR (4–6) are shown: (A) 1×10^6 (1, 4), 3×10^6 (2, 5), and 5×10^6 (3, 6) SPIO-*luc*-mESC are transplanted; (B) *In vivo* correlation between estimated number of transplanted mESC-*luc*$^+$ and the signal area by GRE; and (C) *In vivo* correlation between estimated number of transplanted *luc*-mESC and the signal area by OR. Both linear regression graphs include 95% confidential intervals.

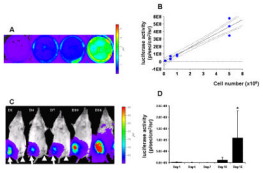

Figure 3. Serial *in vivo* bioluminescence imaging (BLI)

(A) *In vitro* BLI of mESC-luc^{+} demonstrates increasing signal proportionate to the cell quantity (the wells contained 0.1, 0.5, 1, and 5 ×10^{6} *luc*-mESC); (B) *In vitro* correlation between estimated number of *luc*-mESC and BLI activity (linear regression graph includes 95% confidential intervals); (C) *In vivo* BLI shows a representative mice transplanted with *luc*-mESC reporter gene at 1, 4, 7, 10, and 16 days after cell transplantation (arrow: viable cells and arrowhead: non-viable cells); and (D) BLI signal of viable SPIO-*luc*-mESC increased significantly over time by day 16 (*, p<0.001).

Table 1

Linear regression of areas of enhancement and transplanted cell numbers (y=A+Bx), for OR and GRE acquisitions. The uncertainty is one standard deviation.

GRE	A (mm^3)	B($mm^3/10^6$ cells)	R^2	sensitivity, %
	7.4±45.8	93.5±14.4	0.68	30.8
OR	**A (mm^2)**	**B($mm^2/10^6$cells)**	**R^2**	**sensitivity, %**
	9.4±2.1	7.0±0.7	0.79	20.0